·Article·
Advances in Polar Science
doi: 10.3724/SP.J.1085.2012.00204
December 2012 Vol. 23 No. 4: 204-210

Simultaneous optical and radar observations of poleward moving auroral forms under different IMF conditions

XING Zanyang[1, 2*], YANG Huigen[2], HAN Desheng[2], WU Zhensen[1], LIU Junming[2], HU Zejun[2], ZHANG Qinghe[2], LIU Yonghua[2], ZHANG Beichen[2] & HU Hongqiao[2]

[1] School of Science, Xidian University, Xi'an 710071, China;
[2] SOA Key Laboratory for Polar Science, Polar Research Institute of China, Shanghai 200136, China

Received 1 November 2012; accepted 10 December 2012

Abstract Using high temporal resolution optical data obtained from three-wavelength all-sky imagers at Chinese Yellow River Station in the Arctic, together with the EISCAT Svalbard radar (ESR) and SuperDARN radars, we investigated the dayside poleward moving auroral forms (PMAFs) and the associated plasma features in the polar ionosphere under different interplanetary magnetic field (IMF) conditions, between 0900 and 1010 UT on 22 December 2003. Simultaneous optical and ESR observations revealed that all PMAFs were clearly associated with pulsed particle precipitations. During northward IMF, particles can precipitate into lower altitudes and reach the ionospheric E-region, and there is a reverse convection cell associated with these PMAFs. This cell is one of the typical signatures of the dayside high-latitude (lobe) reconnection in the polar ionosphere. These results indicate that the PMAFs were associated with the high-latitude reconnection. During southward IMF, the PMAFs show larger latitudinal motion, indicating a longer mean lifetime, and the associated ionospheric features indicate that the PMAFs were generated by the dayside low-latitude reconnection.

Keywords **PMAFs, polar ionosphere, reconnection**

Citation: Xing Z Y, Yang H G, Han D S, et al. Simultaneous optical and radar observations of poleward moving auroral forms under different IMF conditions. Adv Polar Sci, 2012, 23:204-210, doi: 10.3724/SP.J.1085.2012.00204

0 Introduction

The dayside polar region is where particles, momentum, and energy from solar wind can be transported into the magnetosphere. This coupling process and associated physical courses can map to the polar ionosphere along open magnetic field lines and produce various auroral phenomena. Poleward moving auroral forms (PMAFs) are one of the most common features of the dynamics of dayside polar ionospheric and auroral phenomena[1-9]. These transient forms usually start at the equatorward boundary of the dayside auroral oval and then move poleward, where they fade and finally disappear in the polar cap, several degrees poleward of the auroral oval[1,3]. The PMAFs are frequently observed between 0900 and 1500 MLT, appearing as auroral arcs or arc fragments with lifetimes 2–15 min and recurrence times 3–15 min[2,9].

There are several studies on the mechanisms of dayside PMAFs. Liu and Sibeck[10] suggested that the PMAFs can be caused by solar wind pressure pulses. However, extensive statistical studies have shown that solar wind pressure pulses are not be the main mechanism of PMAFs[2,9]. At present, the PMAFs are widely accepted as typical ionospheric signatures of magnetic reconnection on the dayside magnetopause, in the form of flux transfer events (FTEs). The newly reconnected flux tube is pulled tailward by the solar wind, triggering the PMAF event. Long-term auroral observations show that the majority of PMAFs occur under southward interplanetary magnetic field (IMF) conditions, consistent with the higher reconnection rate at the dayside magnetopause[2,9,11-14]. However, the PMAFs are also relatively frequently observed under northward IMF conditions, which may be associated with the effect of high-latitude

* Corresponding author (email: xingzanyang@pric.gov.cn)

(lobe) reconnection[2,9,13]. In addition, the PMAFs are also influenced by the IMF B_y component and they move along the direction of the magnetic field tension force acting on the newly reconnected flux tubes, which are caused by the magnetic reconnection[2,14-16].

In the present study, we used high temporal resolution auroral data from the Chinese Yellow River Station at Ny-Ålesund, together with data from the EISCAT Svalbard radar (ESR) and SuperDARN radars. We investigated the dayside PMAFs under different IMF conditions during 0900–1010 UT on 22 December 2003. We focused on revealing the various features in auroral forms, auroral movements and ionospheric plasma dynamics associated with different IMF conditions, i.e., northward and southward IMF.

1 Instruments and data

The Chinese Yellow River Station (YRS) is located at Ny-Ålesund, Svalbard in the Arctic. Because of its high geographic latitude (78.92°N), YSR is one of the few ground stations that can make relatively long-term optical auroral observations of the dayside during the boreal winter season. Moreover, since YRS is at 76.24°N corrected geomagnetic latitude, i.e., near the cusp latitude, it is an ideal site for monitoring dayside auroral phenomena, such as PMAFs, and ionospheric responses to various dynamic processes in the dayside magnetospheric boundary layer. An optical observation system[5,17], consisting of three identical all-sky imagers (ASI) with narrow band filters centered at wavelengths 427.8, 557.5 and 630.0 nm, was installed at YSR in November 2003. Since then, continuous optical observations have been made over nine winters using the three ASI. We analyzed auroral data with a high time resolution of 10 s.

The EISCAT Svalbard radar (ESR), located at Longyearbyen, consists of a 32 m steerable antenna and a 42 m antenna. The 42 m antenna is permanently directed parallel to the local geomagnetic field (azimuth 180.6°, elevation 81.6°). The ESR observes the electron density and temperature, ion temperature and ion velocity, and is a powerful tool for investigating plasma flow dynamics. Only data from the field-aligned 42 m antenna are used herein.

The SuperDARN HF radars are designed to investigate field-aligned ionospheric plasma density irregularities and large-scale magnetospheric-ionospheric coupling[18]. Large-scale ionospheric plasma convection maps can be derived from multiple radars using the "map potential" analysis algorithm[19]. We used the Northern Hemispheric SuperDARN data to produce ionospheric convection maps.

The Advanced Composition Explorer (ACE) was launched in August 1997 into a halo orbit around the L1 point to monitor upstream solar wind and IMF conditions. Solar wind data at 64 s resolution from the Solar Wind Experiment and IMF data at 16 s resolution from the magnetometer instrument aboard the ACE spacecraft were also used.

2 Observations

2.1 Solar wind and IMF observations

Figure 1 shows an overview of the solar wind and IMF conditions measured by the ACE spacecraft during 0900–1010 UT on 22 December 2003. From top to bottom, the parameters shown are the three IMF components (B_x, B_y and B_z) in GSM coordinates, IMF clock angle, solar wind plasma number density, solar wind speed, and solar wind dynamic pressure. The data have all been lagged by 44 min. The red horizontal line segments (a–h) mark the time intervals of PMAFs. As seen from Figure 1, at about 0919 UT the IMF B_z component turned from northward to southward, and then remained mainly southward with some short northward turnings. The IMF B_y component was mainly positive with some short negative excursions, and the IMF B_x component was essentially positive over the entire period. The IMF clock angle (defined as positive for rotation from the +Z direction toward +Y) mainly varied between 0° and 180° during this period, except for some large values during the IMF turnings. The solar wind velocity varied between 590 and 640 $km \cdot s^{-1}$ and the solar wind dynamic pressure was around 3 nPa.

2.2 Auroral observations

Figure 2 presents keograms for 427.8 nm, 557.7 nm and 630.0 nm auroral data at YRS during 0900–1010 UT on 22 December 2003, respectively. The keogram for each band is formed by placing the pixel strips continuously, which are extracted along the geomagnetic north-south direction from continuous all-sky images. The keogram represents both latitudinal and temporal variations of emission intensities along the magnetic meridian, and is usually presented as a function of zenith angle and UT. The magnetic latitude corresponding to zenith angle is shown by the right y-axis, assuming maximum heights of auroral emissions at 120 km (427.8 nm), 150 km (557.7 nm) and 220 km (630.0 nm)[5]. PMAFs are identified in the keograms as long poleward moving structures, slanted toward increasing time. According to the criteria described above, eight PMAFs were found during the period of interest, marked by the red bias lines (a–h) in Figure 2. We focused on PMAFs b and c under northward IMF conditions and PMAFs e–h under southward IMF conditions. The IMF experienced polarity turnings during PMAF events a and d. The black dashed line in the bottom panel of Figure 2 shows the equatorward edge of the brightening 630.0 nm aurora, which may be excitated by soft electrons from the magnetosheath and be considered the open-closed boundary of the field line (OCB)[8,20-23]. The approximate location of the ESR with zenith angle 29.06° is marked by the horizontal white line in Figure 2, assuming emission peaked at altitude 220 km[24]. Some PMAFs occurred equatorward of the ESR, and some PMAFs crossed the ESR.

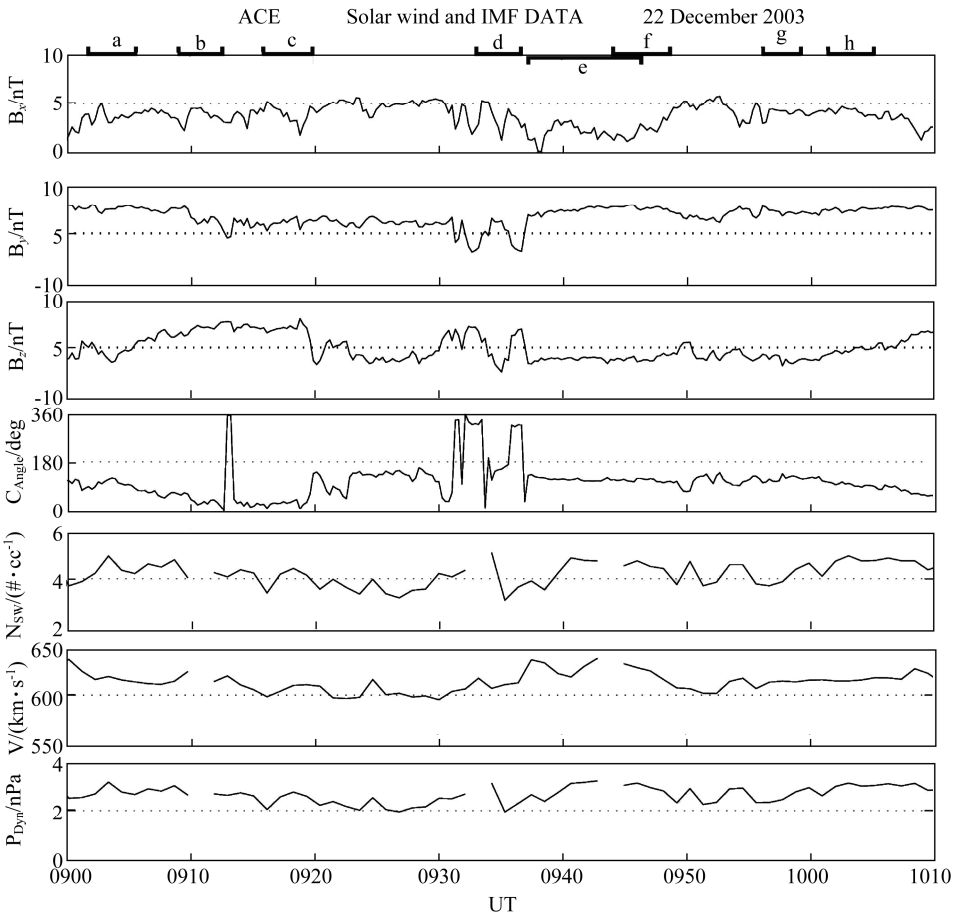

Figure 1 An overview of the solar wind and IMF conditions measured by the ACE satellite between 0900 and 1010 UT on 22 December 2003. Parameters shown: three IMF components (B_x, B_y and B_z) in GSM, IMF clock angle (C_{Angle}), solar wind plasma number density (N_{SW}), solar wind speed (V), and solar wind dynamic pressure (P_{Dyn}).

As seen from Figure 2, the dayside oval was south of the zenith and moved to lower latitude as the IMF was rotated from northward to southward. During the northward IMF, the PMAF intensity at YRS was enhanced at all wavelengths (630.0 nm, 557.7 nm and 427.8 nm). However, during the southward IMF, the auroral intensity decreased and the PMAFs moved to higher latitude and had longer lifetimes.

2.3 ESR observations

Figure 3 shows a multi-panel plot of the electron density (Ne), electron temperature (Te), ion temperature (Ti), and ion line-of-sight velocity (Vi, positive velocities away from the radar), as measured by the field-aligned ESR antenna during 0900–1010 UT on 22 December 2003. This is plotted as a function of altitude (100–800 km) and UT. Figure 3 shows ESR measurements in association with the PMAFs, as marked by the red vertical dotted lines a–h. We clearly see that the ESR recorded elevated and well-structured electron density with concurrent elevated electron temperatures associated with PMAFs, indicating pulsed particle precipitations[25-26]. Events a–d were accompanied by clear enhancements of Ne, which were 2–3 times higher than background electron density, whereas events e–f showed no clear enhancements. This may be caused by two reasons. First, events a–d occurred during a northward IMF or a southward turning just after a northward IMF, which could be associated with high-latitude (lobe) reconnection with low reconnection rate. However, events e–h were observed during a southward IMF or a northward turning after a southward IMF, which is attributable to low-latitude reconnection with a higher reconnection rate. Zhang et al.[27] reported that a number of newly reconnected flux tubes (FTEs) were produced because of the higher reconnection rate during southward IMF, and these convected tailward along the ionospheric convection streamlines at different velocities, so an accumulation could have formed. Thus, electron precipitations in the separated flux tubes could mix with each other and smear the boundary between them (e.g., events e–h, especially events e and h in Figure 3). Second, although the studied interval was on the dayside near local noon (LT=UT+1 h) in midwinter, the atmosphere above 250 km altitude remained sunlit. Hence, the solar EUV ionization would likely result in high-density plasma near or equatorward of the subauroral regions in the polar ionosphere. During a southward IMF, the OCB would leap equatorward to the subauroral reservoir of high-density plasma, followed by a poleward relaxation of that boundary,

carrying the high-density plasma and forming the polar cap patch. This is consistent with expected evolution of the dayside magnetopause reconnection. When the reconnection rate is low, polar cap patches can be easily separated and show high-density and low-temperature plasma in the ESR data (marked with red arrows in Figure 3). When the reconnection rate is high, the accumulated effect and poleward relaxation of the OCB carrying the high-density plasma may lead to enhanced background plasma density, which may weaken the influence of particle precipitations owing to reconnection, and smear the boundaries between them[28].

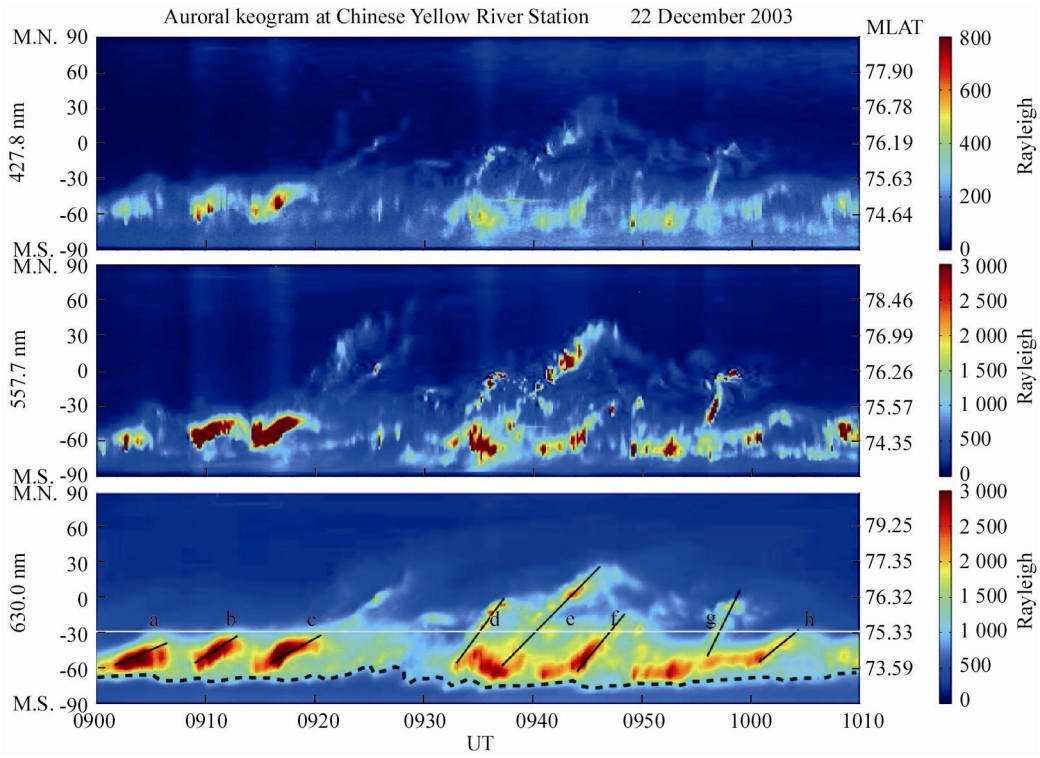

Figure 2 Keograms of auroral observations from three sets of CCD all-sky imagers at YRS during 0900–1010 UT on 22 December 2003. Horizontal white line shows zenith angle of the ESR radar beam with an assumed peak emission altitude of 220 km.

We clearly see that the ESR recorded different ionospheric signatures under the two IMF conditions. During the northward IMF, the enhancements of Ne reached an altitude of 120 km (see events b and c in Figure 3), with concurrent elevated Te (up to 5 000 K). At the same time, the 557.7 nm and 427.8 nm auroral emissions were stronger than those during the southward IMF. These results indicate that the high-energy particles precipitated into the ionospheric E-region. However, during the southward IMF, the enhancements in Ne were at F-region altitudes (> 200 km), with concurrent elevated Te; i.e., low-energy particle precipitations in the F-region. A difference was also identified in ion temperatures (Ti): Ti was less than 1 000 K for northward IMF (lower than background) vs. > 2 000 K for southward IMF (with apparently elevated structures). The enhanced and structured plasma density may result from low-energy particle precipitation, owing to low-latitude reconnection and local Joule heating under southward IMF conditions.

2.4 SuperDARN observations

Figure 4 shows the large-scale convection pattern in the Northern Hemisphere, obtained using the "map potential" algorithm. Flow vectors were derived using SuperDARN velocity measurements. Concentric circles indicate lines of constant magnetic latitude in 10° increments, with noon at the top and dawn to the right in each pattern. The IMF in the Y–Z plane is shown as a red vector, under which the time delay from ACE to the ionosphere is presented in parentheses (44 min). The color and length of the drift vectors indicate convection velocities, with maximum value 1 000 $m \cdot s^{-1}$ in red. The position of YRS is marked by the black dot. As seen in Figure 4, during the northward IMF over the period 0916–0918 UT, the global convection pattern had a complex, multi-cell configuration. A reverse convection cell, one of the typical signatures of dayside high-latitude (lobe) reconnection in the polar ionosphere, was created on the northwest side of YRS. At the same time, PMAF event c was observed near the lobe region governed by anti-sunward flows (Figure 4a). During the southward IMF over the period 0956–0958 UT, convection appeared in an asymmetric two-cell pattern, with the larger one on the dusk side. PMAF event g, as seen by the ASI, occurred on the dusk cell near the cusp region and was dominated by

poleward convection, with increased convection velocities marked by the red vectors. Note that the moving directions of the PMAFs seen by the ASI are consistent with ionospheric flow directions for the northward and southward IMF.

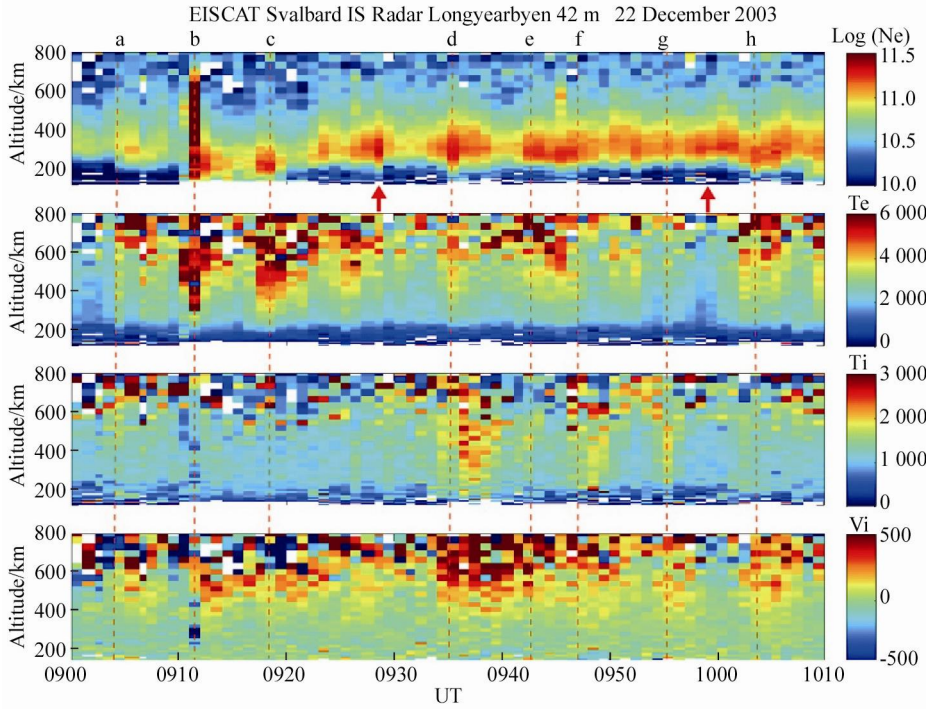

Figure 3 Plasma parameters measured by the field-aligned ESR antenna on 22 December 2003. From top to bottom: electron density (Ne), electron temperature (Te), ion temperature (Ti), and ion line-of-sight velocity (Vi, positive away from radar).

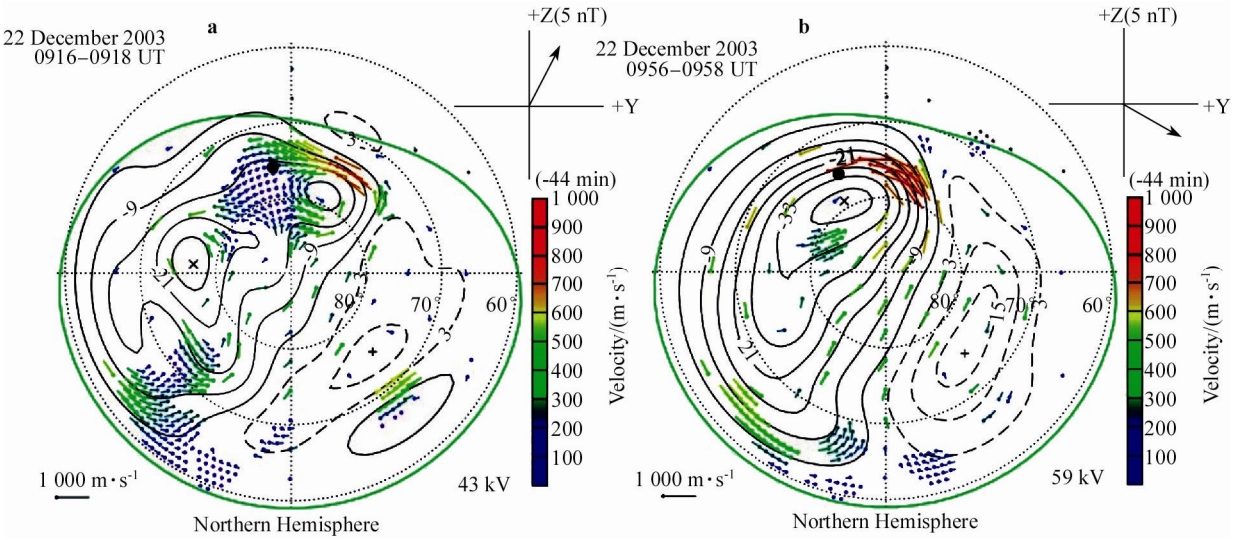

Figure 4 Streamlines and vectors of ionospheric flows derived from the Northern Hemispheric SuperDARN velocity measurements, shown on geomagnetic grids obtained using the "map potential" algorithm. Direction and magnitude of the lagged IMF are indicated at right-hand upper corner of each map. Selected frames cover 2 min scans over 0916–0918 UT (**a**), and 0956–0958 UT (**b**).

3 Discussion

PMAFs are one of the most intensively investigated phenomena in the dayside high-latitude ionosphere, and are commonly interpreted as an ionospheric signature of magnetic reconnection[2-4,6-9,11-15,26-35]. Both case studies and statistical studies based on long-term auroral observations have shown that the majority of PMAFs occurred during southward IMF, suggesting an association with enhanced low-latitude reconnection on the dayside magnetopause. However, previous studies have also found that PMAFs frequently occur during northward IMF conditions, which

suggests lobe reconnection as a possible source[2,9,13]. In the present study, using auroral data obtained from YSR together with the ESR and SuperDARN radars, we investigated in detail the dayside PMAFs associated with different optical and ionospheric features and relevant physical dynamics during northward and southward IMF conditions.

During northward IMF, the auroral oval was at higher latitude; PMAFs moved poleward more slowly and were stronger at 557.7 nm and 427.8 nm auroral emissions than during southward IMF. The elevated and structured electron density observed by ESR reached an altitude of 120 km in the polar ionosphere. These results indicate that high-energy electrons precipitated into the ionospheric E-region, leading to observation of PMAF events. By assuming that the auroral emission (427.8 nm) peaked at altitude 120 km, PMAFs were observed over the ESR beam with zenith angle of 45.21°. Although the ESR was located poleward of the PMAFs, enhancements of Ne and Te were simultaneously observed in the ESR data[30]. As seen from SuperDARN radar observations, we clearly see that a reverse convection cell was created on the northwest side of YSR, and the associated PMAFs seen by the ASI occurred near the antisunward-stream region of the lobe cell, which is considered one of the typical signatures of high-latitude (lobe) reconnection[36-38]. During high-latitude reconnection under northward IMF, lobe-reconnected lines allow auroral precipitation particles to move along streamlines of ionospheric convection, and lead to observations of PMAFs near the lobe region with antisunward-stream flow.

When the IMF turned southward, the auroral oval expanded equatorward because of low-latitude reconnection. There were some channel-like structures in Ne, Te, Ti and Vi, and the associated PMAFs were accompanied by ionospheric ion upflows owing to soft particle precipitation. These features are considered an ionospheric signature of FTEs in the polar ionosphere, generated by low-latitude reconnection on the dayside magnetopause[25-26,39]. As seen from SuperDARN radar data, it is clear that there was an asymmetric two-cell convection pattern distorted by IMF B_y (Figure 4b), and PMAFs seen by the ASI occurred near the antisunward-stream region of the dusk cell. The directions of motion of the PMAFs were consistent with ionospheric flow directions. During low-latitude reconnection under southward IMF, particles in the newly reconnected flux tube pulled tailward by solar wind, precipitated along the magnetic field lines down into the polar ionosphere, triggering the PMAFs.

The PMAFs showed a larger latitudinal motion when the IMF was southward than when it was northward. During the northward IMF, the lobe cell generated by high-latitude reconnection was confined at the dayside high latitude magnetopause, and the associated PMAFs resulting from particle precipitation inside the lobe cell were also confined to this region. However, during the southward IMF, the open field lines resulting from low-latitude reconnection can be pulled into the magnetotail, so the PMAFs can move to higher latitude and have longer lifetimes.

4 Conclusions

We investigated auroral and plasma features of the dayside PMAFs under different IMF conditions, based on high temporal resolution auroral and radar data on 22 December 2003. A series of PMAFs were observed to brighten at the equatorward boundary of the dayside auroral oval, and then propagate poleward under both northward and southward IMF conditions.

From simultaneous optical and ESR observations, we clearly see that all PMAF events were associated with pulsed plasma precipitations. During the northward IMF, high electron density reached an altitude of 120 km, which may be attributed to high energy particles precipitated along the open field lines down into the ionospheric E-region associated with high-latitude reconnection. However, during the southward IMF, high electron density occurred at altitudes greater than 200 km, with apparently elevated Ti associated with ion upflows, which may be attributed to low-energy particle precipitation and Joule heating associated with low-latitude reconnection.

During the northward IMF, the PMAFs observed by the ASI occurred near the antisunward-stream region of the lobe cell associated with high-latitude reconnection. During the southward IMF, the PMAFs occurred near the antisunward-stream region of the dusk cell and moved over a larger latitudinal range because of low-latitude reconnection. In addition, the directions of motion of the PMAFs seen by the ASI were consistent with ionospheric flow directions and the effect of magnetic reconnection.

Acknowledgements This work was supported by the National Natural Science Foundation of China (Grant nos. 40974083, 41031064, 41104091, 41104090, 41274149 and 41274164), the Ocean Public Welfare Scientific Research Project of China (Grant no. 201005017), the Polar Strategic Research Foundation of China (Grant nos. 20100202, 20100203 and 20120304), and the Polar Environment Comprehensive Investigation & Assessment Programs (Grant no. CHINARE 2012-02-03). The auroral data were issued by the Data-sharing Platform of Polar Science(http://www.chinare.org.cn) maintained by PRIC and Chinese National Antarctic & Arctic Data Center. We also acknowledge the ACE, SuperDARN and EISCAT workgroups for supplying the data. The authors thank all members of the Polar Research Institute of China. Many thanks to Prof. Liu Ruiyuan for his useful detailed comments and valuable suggestions.

References

1 Fasel G J, Minow J I, Smith R W, et al. Multiple brightenings of transient dayside auroral forms during oval expansions. Geophys Res Lett, 1992, 19(24): 2429-2432.

2 Fasel G J. Dayside poleward moving auroral forms: A statistical study. J Geophys Res, 1995, 100(A7): 11891-11905.

3 Sandholt P E, Deehr C S, Egeland A, et al. Signatures in the dayside aurora of plasma transfer from the magnetosheath. J Geophys Res, 1986, 91(A9): 10063-10079.

4 Sandholt P E, Farrugia C J. Poleward moving auroral forms (PMAFs) revisited: responses of aurorae, plasma convection and Birkeland currents in the pre- and postnoon sectors under positive and negative IMF By condi-

tions. Ann Geophys, 2007, 25(7): 1629-1652.
5 Hu Z J, Yang H G, Huang D H, et al. Synoptic distribution of dayside aurora: Multiple-wavelength all-sky observation at Yellow River Station in Ny-Ålesund, Svalbard. J Atmos Sol-Terr Phys, 2009, 71(8-9): 794-804. doi: 10.1016/j.jastp.2009.02.010.
6 Lockwood M, Sandholt P E, Cowley S W H. Dayside auroral activity and magnetic flux transfer from the solar wind. Geophys Res Lett, 1989, 16(1): 33-36.
7 Lockwood M, Denig W F, Farmer A D, et al. Ionospheric signatures of pulsed reconnection at the Earth's magnetopause. Nature, 1993, 361(6411): 424-428.
8 Zhang Q H, Dunlop M W, Lockwood M, et al. Simultaneous observations of reconnection pulses at Cluster and their effects on the cusp aurora observed at the Chinese Yellow River Station. J Geophys Res, 2010, 115(A10237), doi:10.1029/2010JA015526.
9 Xing Z Y, Yang H G, Han D S, et al. Poleward moving auroral forms (PMAFs) observed at the Yellow River Station: A statistical study of its dependence on the solar wind conditions. J Atmos Sol -Terr Phys, 2012, 86: 25-33. doi: 10.1016/j.jastp.2012.06.004.
10 Lui A T Y, Sibeck D G. Dayside auroral activities and their implications for impulsive entry processes in the dayside magnetosphere. J Atmos Terr Phys, 1991, 53(3-4): 219-229.
11 Sandholt P E, Farrugia C J, Moen J, et al. Dayside auroral configurations: Responses to southward and northward rotations of the interplanetary magnetic field. J Geophys Res, 1998, 103(A9): 20279-20295.
12 Sandholt P E, Lockwood M, Freeman K S C, et al. Midday auroral breakup events and related energy and momentum transfer from the magnetosheath. J Geophys Res, 1990, 95(A2): 1039-1060.
13 Drury E E, Mende S B, Frey H U, et al. Southern Hemisphere poleward moving auroral forms. J Geophys Res, 2003, 108(A3): 1114. doi: 10.1029/2001JA007536.
14 Karlson K A, Oieroset M, Moen J, et al. A statistical study of flux transfer event signatures in the dayside aurora: The IMF B_y-related prenoon-postnoon asymmetry. J Geophys Res, 1996, 101(A1): 59-68.
15 Sandholt P E, Farrugia C J, Cowley S W H, et al. Dayside auroral bifurcation sequence during B_y-dominated interplanetary magnetic field: Relationship with merging and lobe convection cells. J Geophys Res, 2001, 106(A8): 15429-15444.
16 Sandholt P E, Farrugia C J, Denig W F. Detailed dayside auroral morphology as a function of local time for southeast IMF orientation: implications for solar wind-magnetosphere coupling. Ann Geophys, 2004, 22(10): 3537-3560.
17 Liu R Y, Liu Y H, Xu Z H, et al. The Chinese ground-based instrumentation in support of the combined Cluster/Double Star satellite measurements. Ann Geophys, 2005, 23(8): 2943-2951.
18 Greenwald R A, Baker K B, Dudeney J R, et al. DARN/SuperDARN: A global view of the dynamics of high-latitude convection. Space Sci Rev, 1995, 71(1-4): 761-796.
19 Ruohoniemi J M, Baker K B. Large-scale imaging of high-latitude convection with Super Dual Auroral Radar Network HF radar observations. J Geophys Res, 1998, 103(A9): 20797-20811.
20 Whalen J A, Buchau J, Wagner R A. Airborne ionospheric and optical measurements of noontime aurora. J Atmos Terr Phys, 1971, 33(4): 661-662.
21 Murphree J S, Cogger L L, Anger C D, et al. Large scal 6300Å, 5577Å, 3914Å dayside auroral morphology. Geophys Res Lett, 1980, 7(4): 239-242.
22 Lockwood M, Carlson H C Jr, Sandhold P E. Implications of the altitude of transient 630-nm dayside auroral emissions. J Geophys Res, 1993, 98(A9): 15571-15587.
23 Milan S E, Lester M, Cowley S W H, et al. Meridian-scanning photometer, coherent HF radar, and magnetometer observations of the cusp: a case study. Ann Geophys, 1999, 17(2): 159-172.
24 Sandhold P E, Carlson H C, Egeland A. Dayside and polar cap aurora. Dordrecht, Boston: Kluwer Academic Publishers, 2002: 287.
25 Pitout F, Newell P T, Buchert S C. Simultaneous high- and low-latitude reconnection: ESR and DMSP observations. Ann Geophys, 2002, 20(9): 1311-1320.
26 Moen J, Okasvik K, Carlson H C. On the relationship between ion upflow events and cusp auroral transients. Geophys Res Lett, 2004, 31: L11080. doi: 10.1029/2004GL020129.
27 Zhang Q H, Dunlop M W, Liu R Y, et al. Coordinated Cluster/Double Star and ground-based observations of dayside reconnection signatures on 11 February 2004. Ann Geophys, 2011, 29(10): 1827-1847.
28 Zhang Q H, Zhang B C, Liu R Y, et al. On the importance of interplanetary magnetic field $|B_y|$ on polar cap patch formation. J Geophys Res, 2011, 116(A05308), doi:10.1029/2010JA016287.
29 Hu Z J, Yang H G, Liang J M, et al. The 4-emission-core structure of dayside aurora oval observed by all-sky imager at 557. 7 nm in Ny-Ålesund, Svalbard. J Atmos Sol -Terr Phys, 2010, 72(7-8): 638-642. doi: 10.1016/j.jastp.2010.03.005.
30 Lockwood M, McCrea I W, Milan S, et al. Plasma structure within poleward-moving cusp/cleft auroral transients: EISCAT Svalbard radar observations and an explanation in terms of large local time extent of events. Ann Geophys, 2000, 18(9): 1027-1042.
31 Lockwood M, Moen J. Reconfiguration and closure of lobe flux by reconnection during northward IMF: possible evidence for signatures in cusp/cleft auroral emissions. Ann Geophys, 1999, 17(8): 996-1011.
32 Milan S E, Lester M, Cowley S W H, et al. Dayside convection and auroral morphology during an interval of northward interplanetary magnetic field. Ann Geophys, 2000, 18(4): 436-444.
33 Moen J, Lockwood M, Sandholt P E, et al. Variability of dayside high latitude convection associated with a sequence of auroral transients. J Atmos Terr Phys, 1996, 58(1-4): 85-96.
34 Safargaleev V, Kozlovsky A, Sergienko T, et al. Optical, radar, and magnetic observations of magnetosheath plasma capture during a positive IMF B_z impulse. Ann Geophys, 2008, 26(3): 517-531.
35 Thorolfsson A, Cerisier J C, Lockwood M, et al. Simultaneous optical and radar signatures of poleward-moving auroral forms. Ann Geophys, 2000, 18(9): 1054-1066.
36 Cowley S W H, Lockwood M. Excitation and decay of solar wind-driven flows in the magnetosphere-ionosphere system. Ann Geophys, 1992, 10(12): 103-115.
37 Huang C S, Sofko G J, Koustov A V, et al. Evolution of ionospheric multicell convection during northward interplanetary magnetic field with $|B_z/B_y| > 1$. J Geophys Res, 2000, 105(A12): 27095-27107.
38 Hu H Q, Yeoman T K, Lester M, et al. Dayside flow bursts and high-latitude reconnection when the IMF is strongly northward. Ann Geophys, 2006, 24(8): 2227-2242.
39 Rinne Y, Moen J, Carlson H C, et al. Stratification of east-west plasma flow channels observed in the ionospheric cusp in response to IMF B_y polarity changes. Geophys Res Lett, 2010, 37(L13102), doi:10.1029/2010GL043307.